

R. Scheltema for its construction, and the Stichting voor Fundamenteel Onderzoek der Materie for financial support.

¹I. F. Silvera and J. T. M. Walraven, Phys. Rev. Lett. **44**, 164 (1980).

²I. F. Silvera and J. T. M. Walraven, J. Phys. (Paris), Colloq. **41**, C7-137 (1980); J. T. M. Walraven, I. F. Silvera, and A. P. M. Matthey, Phys. Rev. Lett. **45**, 449 (1980).

³R. W. Cline, T. J. Greytak, D. Kleppner, and D. A. Smith, J. Phys. (Paris), Colloq. **41**, C7-151 (1980).

⁴W. N. Hardy, M. Morrow, R. Jochemsen, B. W. Statt, P. R. Kubik, R. M. Marsolais, A. J. Berlinsky, and A. Lendesman, J. Phys. (Paris), Colloq. **41**, C7-157 (1980), and Phys. Rev. Lett. **45**, 453 (1980).

⁵B. Yurke, D. Ignier, E. Smith, B. Johnson, J. Denker, C. Hammel, D. Lee, and J. Freed, J. Phys. (Paris), Colloq. **41**, C7-177 (1980).

⁶C. E. Hecht, Physica (Utrecht) **25**, 1159 (1959); W. C. Stwalley and L. H. Nosanow, Phys. Rev. Lett. **36**, 910 (1976); L. H. Nosanow, J. Phys. (Paris), Colloq.

41, C7-1 (1980).

⁷I. B. Mantz and D. O. Edwards, Phys. Rev. B **20**, 4518 (1979).

⁸M. Morrow, R. Jochemsen, A. J. Berlinsky, and W. N. Hardy, Phys. Rev. Lett. **46**, 195 (1981).

⁹I. F. Silvera and J. T. M. Walraven, Phys. Rev. Lett. **45**, 1268 (1980).

¹⁰J. T. M. Walraven and I. F. Silvera, Phys. Rev. Lett. **44**, 168 (1980), and J. Phys. (Paris), Colloq. **41**, C7-147 (1980).

¹¹I. F. Silvera and V. V. Goldman, Phys. Rev. Lett. **45**, 915 (1980).

¹²D. O. Edwards and I. B. Mantz, J. Phys. (Paris), Colloq. **41**, C7-257 (1980).

¹³Note that this definition of K_s^{eff} differs by a factor V^{-1} from that in Ref. 9.

¹⁴I. F. Silvera, in Proceedings of the Winter School, Lammi, Finland, January 1979 (unpublished); I. F. Silvera and J. T. M. Walraven, in Proceedings of the European Physical Society Conference on Condensed Matter, Antwerp, Belgium, January 1980 (to be published).

¹⁵B. W. Statt and A. J. Berlinsky, Phys. Rev. Lett. **45**, 2105 (1980).

¹⁶We calculate $A/V = 4$ from Ref. 8.

Lattice-Location Experiment of the Ni-Si Interface by Thin-Crystal Channeling of Helium Ions

N. W. Cheung^(a) and J. W. Mayer^(b)

California Institute of Technology, Pasadena, California 91125

(Received 31 March 1980; revised manuscript received 30 January 1981)

A thin-crystal channeling experiment has been devised to locate preferential sites of monolayers of Ni atoms deposited onto Si crystalline substrates. The Ni scattering yield shows dips or peaks in the angular scan measurements when channeled along the major crystallographic axes and planes of Si. The results can be explained by a dispersed Ni-Si interface with 2.1×10^{15} Ni atoms/cm² occupying the tetrahedral interstitial voids of Si.

PACS numbers: 61.16.-d, 61.80.Mk

Numerous techniques such as low-energy electron diffraction, Auger-electron spectroscopy, X-ray photoemission (XPS), ultraviolet photoelectron spectroscopy, and ion channeling have been applied to the study of metal-semiconductor interfaces.¹⁻⁶ Recently, such studies have revealed that interfaces between metals and semiconductors such as Si, GaSb, InP, and GaAs are chemically reactive even at room temperatures and that the interfaces are far from being abrupt as modeled by various theoretical studies. For the Ni-Si system, the existence of an intermixed interface between as-deposited Ni atoms and the crystalline substrate has been observed by ion channeling for clean Si surfaces prepared under ultrahigh-vacuum conditions as well as chemical-

ly cleaned Si surfaces.⁶ With a coverage of 1×10^{16} Ni atoms/cm², approximately 6×10^{15} Si atoms/cm² are nonregistered with respect to the crystalline (111) substrate. An XPS study has also confirmed the room-temperature reactivity between Ni and Si and the Ni atoms were found to be in a Si-rich environment.^{5,7}

In the present study, a thin-crystal channeling experiment has been devised to locate the lattice sites of monolayers of Ni atoms deposited onto Si crystalline substrates. Ion-beam channeling has been applied to locate preferential sites of impurities in bulk crystals.⁸ By making use of the "flux-peaking" effect of ion channeling, the relative position of the impurity atoms with respect to the host's crystalline matrix can be determined

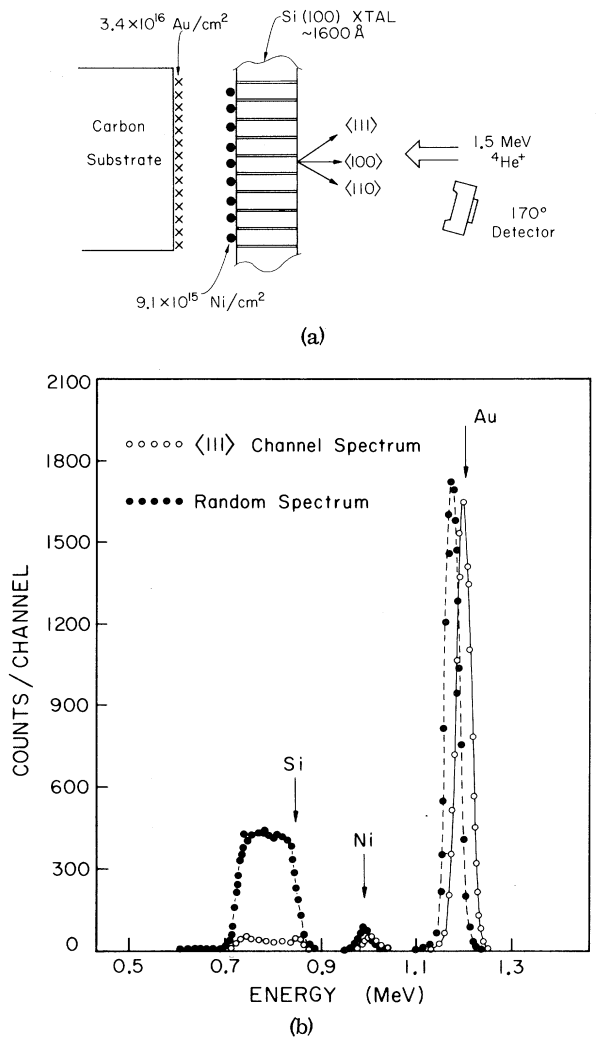


FIG. 1. (a) Experimental setup of the thin-crystal channeling experiment. (b) Channelled and random backscattering spectra showing energy positions of the Si, Ni, and Au signals. The channeling axis is $\langle 111 \rangle$.

by a "triangulation" process, i.e., channeling in different crystallographic directions. Since the establishment of flux peaking requires the beam to traverse $\sim 1000 \text{ \AA}$ into the crystal, this technique is not applicable for impurities located in the near-surface region of bulk crystals. An alternate method based on the blocking effect has been demonstrated by van der Veen *et al.*,⁹ but the technique is only applicable for monolayer or submonolayer impurity coverages. In the case of the thin-crystal experiment, the Si thin crystal ($\sim 2000 \text{ \AA}$ thick) is made self-supporting and the ion beam can enter the crystal via the metal-free surface and establish flux peaking before it en-

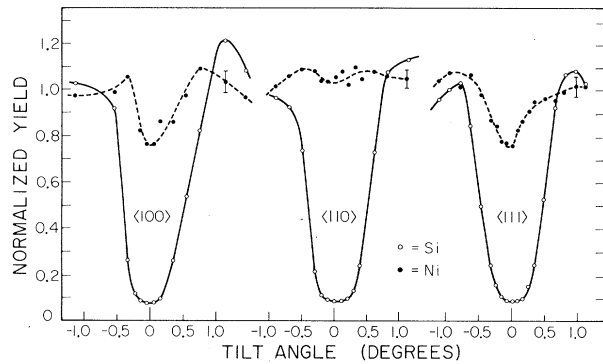


FIG. 2. Angular scan curves of the Si (open circles) and Ni (full circles) total scattering yields, normalized by the Au yield, along the $\langle 100 \rangle$, $\langle 110 \rangle$, and $\langle 111 \rangle$ axes. The random yields are defined to be unity.

counters the Ni-Si interface at the exit side of the thin crystal.

The experimental setup is illustrated in Fig. 1(a). The Si (100) crystal used is about 1600 \AA thick and is $\sim 1 \text{ cm}$ in diam. It is made self-supporting by a chemical etching technique.¹⁰ Prior to Ni evaporation, the crystal was organically degreased and etched in hydrofluoric acid. Such a surface treatment will leave $\leq 1 \times 10^{15}$ oxygen atoms/cm² and $\leq 5 \times 10^{14}$ carbon atoms/cm² on the Si surface as measured by nuclear resonance techniques. The monolayer(s) of contaminants apparently does not block the interdiffusion of Ni and Si atoms as reported in Ref. 6. The Ni deposition was performed in an electron-beam evaporation system with a residual gas pressure of 4×10^{-8} Torr. Approximately 10^{16} Ni/cm² were deposited onto the Si crystal. This coverage is of the order needed to complete the intermixed interfacial region as established from previous channeling experiments.⁶

The Si thin crystal was then mounted on a tilt-plus-rotation goniometer with the metal-free surface facing the helium ion beam (1.5 MeV). The detector was placed at 170° scattering angle, and the total Ni scattering yield was normalized by the total scattering yield from an Au layer on a carbon substrate placed behind the thin crystal.

The $\langle 111 \rangle$ -channelled and random spectra of the Si crystal with a Ni coverage of 9.1×10^{15} atoms/cm² are shown in Fig. 1(b). Both the Au and Ni signals appear at slightly higher energies for the channelled spectrum because of the anomalously low energy loss of the channelled particles. In Fig. 2, the normalized Si and Ni scattering yields

are plotted as a function of the tilt angle around the $\langle 100 \rangle$, $\langle 110 \rangle$, and $\langle 111 \rangle$ axes. The error bars as indicated in the figure are probable statistical fluctuations. Angular dips of $\sim 23\%$ of the Ni signal are observed along the $\langle 100 \rangle$ and $\langle 111 \rangle$ axes. For the $\langle 110 \rangle$ axis, two shoulderlike structures are observed for the Ni angular scan curve and the channeled yields are slightly higher than the random yields for tilt angles less than the channeling critical angle. With use of this triangulation process, it is evident that preferential sites do exist for the Ni atoms. The magnitude of the dips along the $\langle 100 \rangle$ and $\langle 111 \rangle$ axes both correspond to an areal density of 2.1×10^{15} Ni atoms/cm². In Fig. 3, the normalized Ni and Si scattering yields are plotted as a function of the tilt angle along the (100), (110), and (111) planar channeling directions. For (100) planar channeling, the Ni angular scan curve shows a small dip. An angular dip of $\sim 23\%$ is again observed along the (110) planar channeling direction whereas a peak is observed for the angular scan curve along the (111) planar channeling direction.

From these channeling results, it is important to point out that the preferential sites of the Ni atoms are incompatible with any of the crystal structures of nickel silicides such as Ni₂Si, Ni₃Si₂, NiSi, and NiSi₂. Since angular dips have been observed only in the $\langle 100 \rangle$ and $\langle 111 \rangle$ but not the $\langle 110 \rangle$ channeling direction, the possibility of having the preferential sites being epitaxial Ni (fcc structure) on Si or the Ni atoms being in substitutional sites of Si can also be excluded. Instead, the channeling data can be explained by having $\sim 2.1 \times 10^{15}$ /cm² of Ni atoms being located at the tetrahedral sites of the crystalline matrix. Inside a perfect Si crystal, large interstitial voids are formed by Si cages consisting of ten Si atoms hav-

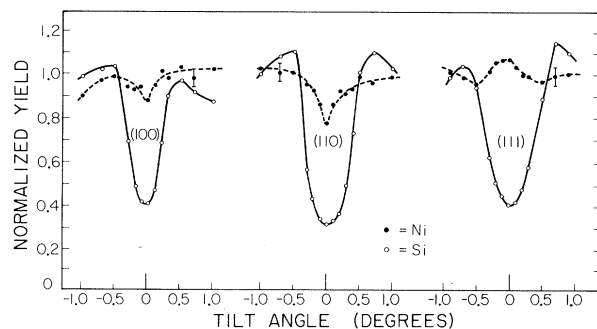


FIG. 3. Angular scan curves of the Si (open circles) and Ni (full circles) total scattering yields, normalized by the Au yield, along the (100), (110), and (111) planes.

ing the "adamantane" structure.¹¹ Such a cage is illustrated in Fig. 4(a), with six of the Si atoms taking up vertices of an octahedron (B sites) and four Si atoms taking up the vertices of a tetrahedron (A sites). The Si-Si bonds are depicted as tapered arrows in the diagram. With the Ni atoms situated at the center of the polyhedron, the projections of the sites along various channeling directions are shown in Fig. 4(b). "Shadowing" of tetrahedral sites by the Si host atoms is found along the $\langle 100 \rangle$ and $\langle 111 \rangle$ axial, and (100) and (110) planar channeling directions. Along the $\langle 100 \rangle$ axial and (111) planar channeling directions, the tetrahedral sites will be exposed to the channeled beam and the channeled scattering yields are expected to be higher than the random scattering yields.

The results could also be explained by having three monolayers of Ni arranged in a diamond lattice on top of the Si (100) surface and registered with respect to the tetrahedral sites of the underlying Si substrate.¹² Such a lattice arrangement and registration is highly unlikely because of the presence of an interfacial mixed layer where the nonregistered Si has disrupted the crystallinity of the Si matrix. We believe that the interstitial Ni is located below the surface in the tail of the Ni distribution within the crystalline portion of the interfacial layer. The interstitial Ni will be surrounded by ten Si nearest neighbors; a site that is consistent with the energy shift of Ni 2P_{3/2} signal of the XPS studies.⁷ The channeling half-angles ($\psi_{1/2}$) of the Ni yield are considerably

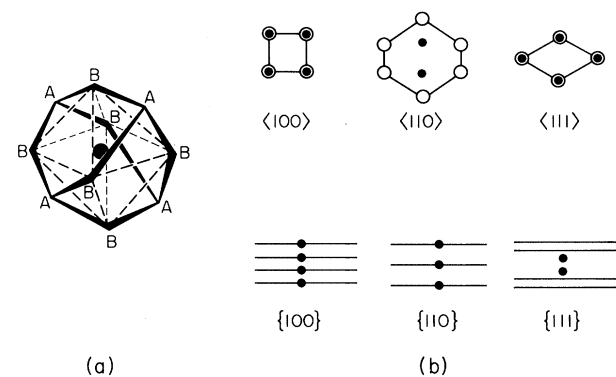


FIG. 4. (a) The adamantane structure of the Si cages inside a Si crystal. The tetrahedral site is depicted by the full circle at the center of the polyhedra. (b) Projected positions of the tetrahedral sites (full circles) along the various major channeling directions of the diamond lattice. The Si atomic rows are represented by open circles and the Si atomic planes are represented by solid lines.

smaller than those of the Si host atoms and the flux-peaking effect is less prominent than theoretical predictions.¹³ For axial channeling, the ratio of the channeling half-angles ($\psi_{1/2}^{\text{Ni}}/\psi_{1/2}^{\text{Si}}$) is about $\frac{2}{3}$ and the ratio decreases to $\frac{1}{2}$ for planar channeling. These observations suggest that the Ni atoms at the tetrahedral sites are not exactly in registry with the Si bulk crystalline matrix. To obtain a rough estimation of the lateral displacements of the Ni atoms, the transverse kinetic energy of the incident beam at $\psi_{1/2}^{\text{Ni}}$ is equated to Lindhard's continuum potential at a distance r from the Si atomic rows,¹⁴

$$E(\psi_{1/2}^{\text{Ni}})^2 = U(r) = \frac{Z_1 Z_2 e^2}{d} \ln \left\{ \left(\frac{\sqrt{3}a}{r} \right)^2 + 1 \right\}. \quad (1)$$

From the $\langle 100 \rangle$ and $\langle 111 \rangle$ angular scan curves, the values of $\psi_{1/2}^{\text{Ni}}$ are 0.34° and 0.38° , respectively, and they both give a value of $\sim 0.3 \text{ \AA}$ for r . The displacement value agrees with the strain between the interstitial Ni atom and atoms of the Si cage if a hard-sphere model is used. In addition, the planar channeling results also show the effects of such displacements by having a smaller dip along the (100) planes ($d_p = 1.36 \text{ \AA}$) than the (110) planes ($d_p = 1.92 \text{ \AA}$).

Tu¹⁵ has postulated an interstitial diffusion mechanism at the metal-silicon interface to explain the low-temperature formation of near-noble metal silicides. Walser and Bené¹⁶ have also proposed an interfacial model with the interfacial region being amorphous and having the lowest eutectic composition to explain the first silicide phase being nucleated. For the Ni-Si system, the present channeling results show that interstitial Ni atoms exist in a strained crystalline matrix. If a structureless interfacial region does exist, it is reasonable to assume that such a region has to occur between the interstitial Ni layer and the metal or silicide layer.

The authors would like to thank Dr. L. C. Feldman (Bell Laboratories) and Dr. W. K. Chu (IBM)

for many helpful discussions. This research was supported in part by the U. S. Office of Naval Research.

^(a)Permanent address: Department of Electrical Engineering and Computer Sciences, University of California, Berkeley, Cal. 94720.

^(b)Permanent address: Department of Material Science and Engineering, Cornell University, Ithaca, N.Y. 14853.

¹J. L. Freeouf, G. W. Rubloff, P. S. Ho, and T. S. Kuan, Phys. Rev. Lett. **43**, 1836 (1979).

²W. E. Spicer, J. Lindau, P. Skeath, C. Y. Su, and P. Chye, Phys. Rev. Lett. **44**, 420 (1980).

³J. N. Miller, S. A. Schwarz, I. Lindau, W. E. Spicer, B. De Michelis, I. Abbati, and L. Braicovich, J. Vac. Sci. Technol. **17**, 920-923 (1980).

⁴L. Braicovich, I. Abbati, J. N. Miller, I. Lindau, S. A. Schwarz, P. R. Skeath, C. Y. Su, and W. E. Spicer, J. Vac. Sci. Technol. **17**, 1005-1008 (1980).

⁵P. J. Grunthaner, F. J. Grunthaner, and J. W. Mayer, J. Vac. Sci. Technol. **17**, 924-929 (1980).

⁶N. W. Cheung, R. J. Culbertson, L. C. Feldman, P. J. Silverman, K. W. West, and J. W. Mayer, Phys. Rev. Lett. **45**, 120 (1980).

⁷N. W. Cheung, P. J. Grunthaner, F. J. Grunthaner, J. W. Mayer, and B. M. Ullrich, to be published.

⁸For example, see S. T. Picraux, in *New Uses of Ion Accelerators*, edited by J. F. Ziegler (Plenum, New York, 1975), p. 229.

⁹J. F. van der Veen, R. M. Tromp, R. G. Smeenk, and F. W. Saris, Surf. Sci. **82**, 468 (1979).

¹⁰N. W. Cheung, Rev. Sci. Instrum. **51**, 1212 (1980).

¹¹F. A. Cotton and G. Wilkinson, *Advanced Inorganic Chemistry* (Wiley, New York, 1972), p. 35.

¹²The tetrahedral sites of Si also form a diamond lattice with the same lattice constant as Si.

¹³S. T. Picraux, W. L. Brown, and W. M. Gibson, Phys. Rev. B **6**, 1382 (1972).

¹⁴J. A. Davies, in *Channeling-Theory, Observations, and Applications*, edited by D. V. Morgan (Wiley, New York, 1973), p. 391.

¹⁵K. N. Tu, Appl. Phys. Lett. **27**, 221 (1975).

¹⁶R. M. Walser and R. W. Bené, Appl. Phys. Lett. **28**, 629 (1976).